

# A Numerical Investigation of Flow Rate Effect on Vortices in Intake Sump

B. SHIN<sup>a)</sup>

## Abstract

The effect of the flow rate on free surface vortices in pump sump was investigated by numerical approach. Free surface flow in an intake channel was solved by using finite volume method for RANS equations with  $k-\omega$  SST turbulence model. A VOF multiphase model and the open channel model were used to solve the multiphase flow in the sump. Minimum level of air-water interface and iso-surfaces of vortices were used to identify the location and shape of the free surface as well as surface vortices. By monitoring the air-water interface with varying flow rate, it was found that when the flow rate increased, more free surface vortices appeared. The formation mechanism of free surface vortices and the pulling air bubbles as well as the development process of vortices were clarified by using the volume rendering method and air volume fraction contours. The locations of the center core of air-entrained vortices on the free surface were in good agreement with those of experiments.

**Keywords:** Numerical analysis, VOF multiphase model, Minimum level of air-water interface, Vortex behavior

## 1. INTRODUCTION

When a vortex enters a pump, the impeller blade encounters the abnormal fluctuating pressure and load, resulting in mechanical unbalance, vibration, noises and acceleration of mechanical wear<sup>1)</sup>. Moreover, the low pressure can be decreased enough to generate cavitation and damage the impeller blades. Consequently, they lead to a clear reduction in pump performance, loss of efficiency, and increased operating costs. These problems are related to certain undesirable flow characteristics in the pump sump, and are caused mainly by poor design of the intake structure layout or insufficient pump inlet bell submergence. Particularly, in situations which continuously require to consider lower construction costs and more compact size, the chances of geometrical problems arising increases<sup>2)-3)</sup>.

Therefore, in order to make an advanced design of the pump sump preventing adverse flow conditions and to get detailed flow information, a great deal of experimental work has been carried out<sup>4)-5)</sup>. Such model test by experimental approaches, however, involves many limitations on the modification of the geometry and the variation of test options. Fortunately, with the progress in computational environment and rapid propagation of computational fluid dynamics (CFD), many numerical approaches to predict the flow in pump sumps recently have been attempted<sup>1),6)-7)</sup>. CFD is being regarded as a suitable alternative for evaluating sump performance and contributed to improve the flow condition for the optimum design of pump sump. Nevertheless, the behavior of free

surface vortices has not been satisfactorily clarified in most CFD studies because they computed the free surface flow under the assumptions such as the flat free surface or fixed slip wall without friction and a single phase problem. In the simulation of the sump flow, therefore, it has to pay attention to the treatment of the free surface because due to the mutual interactions between gas and liquid phases, the free surface flow strongly influences the generation and decay of surface vortices in a real sump construction. The consideration of multiphase flow models also needs to simulate multiphase flows associated with air entrainment.

In this paper, a numerical simulation of 3-D free surface flows in pump intake sump is carried out to investigate the behavior of surface vortices with respect to the flow rate. A finite volume method is used to solve RANS equations with  $k-\omega$  SST turbulence model. A volume of fluid (VOF) multiphase model and an open channel model are applied to analyze the free surface flow problem with accurate. By using the iso-surface contour of air-water interfaces and air-entrained vortices, velocity vectors and streamlines, the behavior of the free surface and surface vortices is investigated and discussed.

## 2. COMPUTATIONAL MODEL

The sump model for computation is a single pump-intake configuration as shown in Fig.1. It was designed based on the recommendation of HI-9.8 Standard<sup>8)</sup> for a single rectangular intake channel. In this figure, the inlet bell mouth diameter  $D$  was used as the basic design parameter. The intake pipe with the inside di

a) Professor, Dept. of Mechanical Design Systems Engineering.

iameter  $d$  of  $0.6D$  is located in the middle of intake channel width  $W$  ( $=2D$ ) at a distance  $B$  of  $0.75D$  from the back wall to the pump inlet bell center. Thickness of the intake pipe and bell was taken by  $0.04D$ .  $E$  denotes intake channel height adjustable according to the water level  $H$ . A fixed value of the bottom clearance  $C$  from floor is equal to  $0.4D$ . The length  $L$  of rectangular intake channel is  $7.32D$ . The submergence  $S$  is defined by  $H-C$ . The origin of coordinates was located at the center of the bell mouth on the floor.

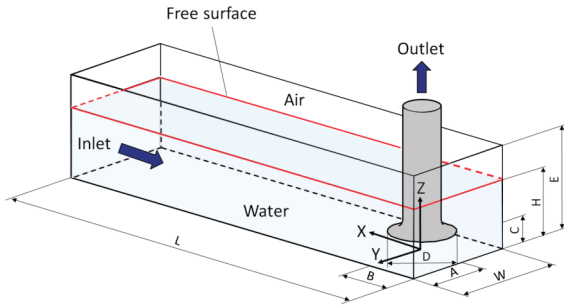


Fig. 1. Schematic illustration of sump model and dimensions.

### 3. COMPUTATIONAL METHOD

Numerical analysis of 3-D multiphase flow in a pump suction sump was done by using the finite volume method incorporated in a CFD code Fluent<sup>9</sup>.  $k-\omega$  SST turbulence model which seems to be an appropriate model to compute the real flow field<sup>10</sup>, and VOF multiphase model were used to solve the problem of multiphase turbulence flow in the open channel. The fundamental equations are the continuity equation and the RANS equations expressed as

$$\frac{\partial \rho}{\partial t} + \frac{\partial}{\partial x_j}(\rho u_j) = 0 \quad (j = 1, 2, 3) \quad (1)$$

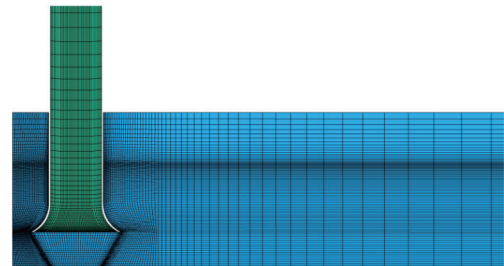
$$\begin{aligned} \frac{\partial \rho u_i}{\partial t} + \frac{\partial}{\partial x_j}(\rho u_i u_j) = - \frac{\partial p}{\partial x_i} \\ + \frac{\partial}{\partial x_j} \left[ \mu_{eff} \left( \frac{\partial u_i}{\partial x_j} + \frac{\partial u_j}{\partial x_i} \right) \right] + f_i^b + f_i^v \end{aligned} \quad (i, j = 1, 2, 3) \quad (2)$$

where  $\rho$ ,  $u$  and  $p$  refer to fluid density, velocity and static pressure, respectively.  $t$  is the time and  $\mu_{eff}$  is the effective viscosity considered molecular viscosity and turbulent viscosity.  $f_i^b$  is the body force (gravity in this case), and  $f_i^v$  is the volumetric tension force to consider the effects of surface tension at fluid-fluid

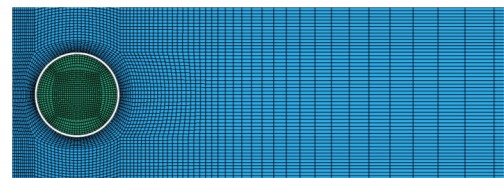
interface. A conservation equation of air volume fraction is solved to capture the air-water interface, and the second order discretization was used in all derivatives.

In this computation, the Dirichlet boundary condition of pressure was imposed on the inlet boundary with the law of hydrostatics. The boundary condition of mass flow rate was used for the outlet with its respective values referred to Table 1. The top plane of air phase was set to a pressure boundary condition with zero atmospheric gauge pressure. On the boundary between the air and water interface, an open channel model which is combined with the VOF model in the Fluent and suitable for the free surface flow problem was applied so that it can accurately capture the air-water interface and flow interactions between phases. The remaining parts of the present sump model were set to no-slip walls in the turbulent flow problem. For the cells near the interface between air and water phases, the geometric reconstruction scheme was utilized to capture the interface sharply. The working liquid is city water at 20°C.

The computational grid was generated by ICEM CFD<sup>11</sup>. A multi-block structured hexahedral grid with high density at the free surface region was generated to capture the sensitive behaviors of the fluid-fluid interface as shown in Fig.2(a). An O-type structured fine mesh near bell mouth and intake pipe (Fig.2(b)) was used to capture the boundary layer with accurate. As a result of the GCI<sup>12</sup> estimation, the grid had 851,000 hexahedral elements was used in all simulations of this study.



(a) High density mesh near free surface (side view)

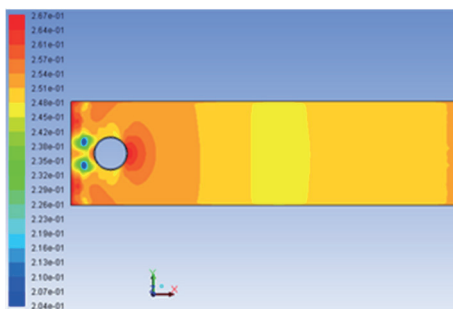


(b) O-grid structure around bell mouth and intake pipe (bottom view)

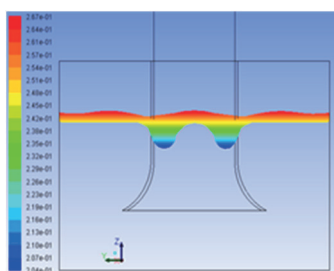
Fig. 2. Computational grid near intake pipe.

### 4. NUMERICAL RESULTS

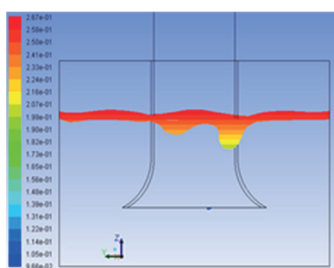
Figure 3 shows a time evolution of the air-entrained vortex she and the air-water interface indicated by  $z$ -coordinate near the intake pipe at water level of  $1.0D$  and flow rate of  $190.35\text{m}^3/\text{h}$ . At early stage of operation,  $T = t_0$ , almost symmetric a pair of free surface vortices occurred behind the suction pipe (Fig.3 (b)), and then the shape of vortices was changed to an asymmetric pattern due to the flow instability and mutual interaction of two vortices. The vortex greater in depth and strength moved gradually to the right hand side of the channel with time as illustrated in Fig.3 (c), and the vortices slightly shrank due to the break-off of the free surface vortices in Fig.3 (d). In addition, because the narrow space between the intake pipe and the back wall influences the normal development of these vortices as shown in Fig.3 (a), the shape of vortex is shown somewhat differently from the conventional vortex occurring behind the cylinder. Relatively weak corner vortices were observed at the both corners of sump channel as well.



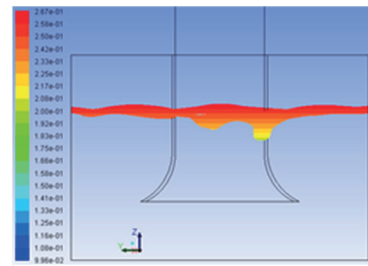
(a)  $T = t_0$  (top view)



(b)  $T = t_0$  (front view)



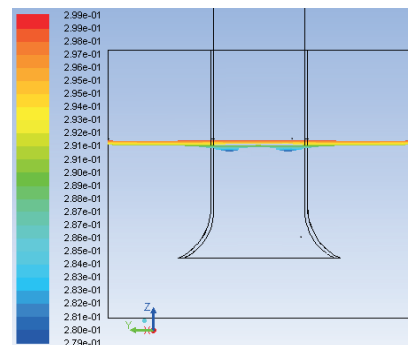
(c)  $T = t_0 + 20\text{s}$



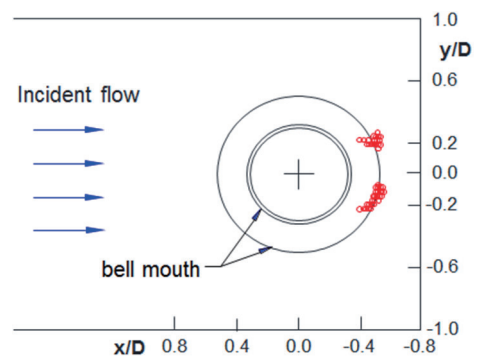
(d)  $T = t_0 + 40\text{s}$

Fig. 3. Time evolution of vortex shape and air-water interface indicated by  $z$ -elevation at  $H=1.0D$  and  $Q = 190.35\text{m}^3/\text{h}$ .

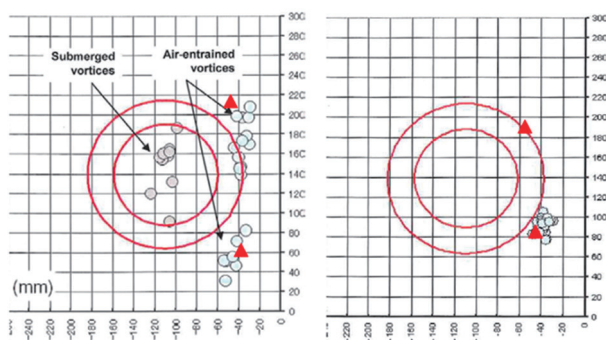
In order to investigate the effect of flow rate on the free surface vortex, numerical simulations with different flow rates at water level of  $1.2D$  was performed. Figure 4(a) shows an instantaneous location of air-water interface with free surface vortices near intake pipe at flow rate of  $126.90\text{m}^3/\text{h}$ . At relatively low flow rates, two nearly symmetrical free surface vortices appeared. Compared to the previous case in Fig.3, the time variation of vortices was rather stable and symmetric pattern remained for a long time. The vortex core of the vortices was mostly located at around  $\pm 0.2y/D$  behind the intake pipe as illustrated in Fig.4(b), and the location qualitatively agreed well with the experimental data represented by symbol “ $\circ$ ” and other existing results by solid symbol “ $\blacktriangle$ ”<sup>13</sup> in Fig.4(c).



(a) Air-water interface



(b) Present prediction



(c) Experimental data

Fig. 4. Instantaneous location of air-water interface presented by z-coordinate and vortex core.

Figure 8 shows time averaged minimum level of the air-water interface. As mentioned above, the minimum level was decreased with the flow rate. That is, when flow rate was increased gradually from  $126.9\text{m}^3/\text{h}$  to  $237.94\text{m}^3/\text{h}$ , the minimum level of the free surface decreased correspondingly, for all the water levels examined in this study.

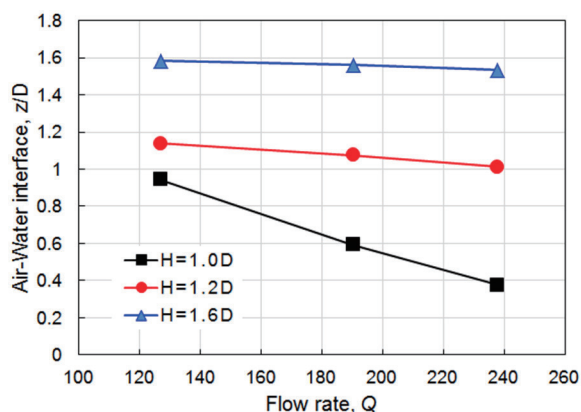


Fig. 5. Time averaged minimum level of the air-water interface.

## 5. CONCLUSION

A numerical study of 3-D free surface vortices formed around the intake pipe in pump sump was performed by using RANS equations and  $k-\omega$  SST turbulence model. A VOF multiphase model and a multi-block structured grid were used. The open

channel boundary conditions were imposed to solve a free surface flow problem with accurate. A single intake channel flow with variation of flow rate was computed and investigated. Conclusions are summarized as follows.

From the measurement of the minimum level of air-water interface and the minimum position of air bubbles, the behavior and shape of free surface vortex corresponding to each case of given flow rates were clearly identified. By monitoring the air-water interface with variation of flow rates, it was confirmed that the flow rate has a significant effect on the occurrence of free surface vortex. It showed that the larger flow rate increased the appearance of the surface vortices. The predicted locations of the air-entrained vortex core on the free surface were in a good agreement with those of experiments.

## REFERENCES

- Constantinescu, G.S. and Patel, V.C., Role of Turbulence Model in Prediction of Pump-Bay Vortices, *J. Hydraul. Eng.*, Vol.126 (2000), pp. 387-391.
- Funaki, J., et al., Flow Measurements in a Suction Sump by UVP, *JSME J. Fluid Sci. and Tech.*, Vol.3 (2008), pp. 68-79.
- Okamura, T., Kamemoto, K. and Matsui, J., CFD Prediction and Model Experiment on Suction Vortices in Pump Sump, *Proc. 9th Asian Int. Conf. on Fluid Machinery*, Jeju, 2007, AICFM9-053.
- Nagahara, H., Sato, T., and Okamura, T., Measurement of the Flow around the Submerged Vortex Cavitation in a Pump Intake by means of PIV, *Proc. 5th Int'l Sympo. On Cavitation*, Osaka, 2003.
- Yildirim, N., Eyupoglu, A., and Tastan, K., Critical Submergence for Dual Rectangular Intakes, *J. Energy Eng.*, Vol.138 (2012), pp. 237-245.
- Constantinescu, G.S. and Patel, V.C., Numerical Model for Simulation of Pump-Intake Flow and Vortices, *J. Hydraul. Eng.*, Vol.126 (1998), pp. 123-134.
- Mohd. Remy Rozainy, et al., Application of Computational Fluid Dynamics (CFD) in Physical Model of Pump Sump to Predict the Flow Characteristics, *Proc. Int. Conf. Const. and Build. Tech.*, Kuala Lumpur, 2008, pp. 79-90.
- Claxton, J., et al., American National Standard for Pump Intakes Design, Hydraulic Institute, ANSI/HI 9.8, 1998.
- ANSYS group, FLUENT User's Manual, Ver. 13, 2010.
- Issa, A., Bayeul-Laine, A.C. and Bois, G., Numerical Simulation of Flow Field Formed in Water Pump-Sump, *Proc. 24th IAHR Symp. on Hydraul. Machinery Systems*, Iguassu, 2008.
- ANSYS group, ICEM CFD User's Manual, Ver. 13, 2010.
- Roache, P.J., Perspective: A Method for Uniform Reporting of Grid Refinement Studies, *ASME J. Fluids Eng.*, Vol.116 (1994), pp. 405-413.
- Zhao, L.J. and Nohmi, M., Numerical simulation of free water surface in pump intake, *Proc. 26th IAHR Symp. on Hydraul. Machinery Systems*, Beijing, 2012.